Comparitive analysis of an automotive air conditioning systems operating with CO_2 and R134a

J. Steven Brown[a], Samuel F. Yana-Motta[b], Piotr A. Domanski[c],*

[a]*Catholic University of America, Washington, DC, USA*
[b]*Formerly NIST, presently Honeywell International Inc., Buffalo, NY, USA*
[c]*National Institute of Standards and Technology, Gaithersburg, MD, USA*

Abstract

This paper evaluates performance merits of CO_2 and R134a automotive air conditioning systems using semi-theoretical cycle models. The R134a system had a current-production configuration, which consisted of a compressor, condenser, expansion device, and evaporator. The CO_2 system was additionally equipped with a liquid-line/suction-line heat exchanger. Using these two systems, an effort was made to derive an equitable comparison of performance; the components in both systems were equivalent and differences in thermodynamic and transport properties were accounted for in the simulations. The analysis showed R134a having a better COP than CO_2 with the COP disparity being dependent on compressor speed (system capacity) and ambient temperature. For a compressor speed of 1000 RPM, the COP of CO_2 was lower by 21% at 32.2°C and by 34% at 48.9°C. At higher speeds and ambient temperatures, the COP disparity was even greater. The entropy generation calculations indicated that the large entropy generation in the gas cooler was the primary cause for the lower performance of CO_2. © 2001 Elsevier Science Ltd and IIR. All rights reserved.

Keywords: Air conditioning; Automobile; CO_2; R134a; Performance

Analyse d'un système de conditionnement d'air automobile utilisant du dioxyde de carbone et du R134a

Résumé

Cette communication évalue les performances des systèmes de conditionnement d'air automobiles utilisant du dioxyde de carbone (CO_2) et du R134a, à l'aide de modèles quasi-théoriques de cycles. Le système au CO_2 était équipé d'un échangeur de chaleur liquide/vapeur à l'aspiration. Les auteurs ont étudié ces deux systèmes afin de comparer les performances de façon fiable ; les composants des systèmes étaient les mêmes et les différences, en termes de propriétés thermodynamiques et de transport, ont été décelées. L'analyse a montré que le R134a possède un meilleur COP que le CO_2, et que la différence entre les COP est fonction de la vitesse du compresseur (puissance du système) et de la température ambiante. Pour une vitesse du compresseur de 1000 tours par minute, le COP du CO_2 a été inférieur de 21% à 32,2°C et de 34% à 48,9°C. A des vitesses et des températures ambiantes plus élevées, cette différence a été encore plus marquée. Les

---

* Corresponding author. Tel.: +1-301-975-5877.
  E-mail address: piotr.domanski@nist.gov (P.A. Domanski).

calculs montrent que la génération importante d'entropie dans le refroidisseur à gaz était la cause principale de la performance réduite du système au CO_2.

Mots clés : Conditionnement d'air ; Automobile ; CO_2 ; R134a ; Performance

---

Nomenclature

A	area (m^2)
b	coefficient defined in Eqs. (6) and (A2)
COP	coefficient of performance
c_p	specific heat at constant pressure (kJ kg^{-1} K^{-1})
$\overline{cp}$	function defined in Eq. (6) (kJ kg^{-1} K^{-1})
c_v	specific heat at constant volume (kJ kg^{-1} K^{-1})
f	friction factor
i	specific enthalpy (kJ kg^{-1})
llsl-hx	liquid-line/suction-line heat exchanger
$\dot{m}$	mass flow rate (kg s^{-1})
Nu	Nusselt number
P	pressure (kPa)
Pr	Prandtl number
$\dot{Q}$	heat transfer rate (kW)
R	resistance to heat transfer (K kW^{-1})
RPM	revolutions per minute
Re	Reynolds number
s	specific entropy (kJ kg^{-1} K^{-1})
T	temperature (°C)
TEWI	total equivalent warming impact
U	overall heat-transfer coefficient (m^2 K kW^{-1})

Greek letters

γ	specific heat ratio (c_p/c_v)
η	efficiency
θ	pressure ratio
ρ	density (kg m^{-3})
ξ	Flonenko friction factor, Eq. (8)

Subscripts and superscripts

b	bulk
cr	critical
HTF	external heat-transfer fluid
hx	heat exchanger
j	defined in Eqs. (6) and (A3)
n	defined in Eqs. (6) and (A1)
PK	Petukhov–Kirillov
q	defined in Eq. (6)
r	refrigerant
s	isentropic
tube	tube
V	volumetric
w	wall

1. Introduction

In response to the Montreal Protocol and consequent regulations, the air-conditioning industry is now in the process of evaluating and introducing new refrigerants as replacements to chlorofluorocarbons (CFCs) and hydrochlorofluorocarbons (HCFCs). In the automotive sector, the transition to a chlorine-free refrigerant took place in the early 1990's when R134a (hydrofluorocarbon, HFC) replaced R12 (CFC). Increasing concerns about global warming brought about an opinion that R134a should not be used long-term because of its global warming potential (GWP), which is 1300 times that of carbon dioxide. Research interests turned to fluids with a low GWP with particular attention given to carbon dioxide as a candidate for automotive applications. The objective of a significant part of this research effort has been to demonstrate that a carbon dioxide system can have a comparable coefficient of performance (COP) to that of an R134a system. A similar level of efficiency for carbon dioxide is very important because a refrigerant's environmental impact on climate change is determined not only by the refrigerant's trapping of infrared radiation (direct effect indicated by the GWP) but also by trapping of infrared radiation by carbon dioxide that is released upon burning of fossil fuels needed to power the air conditioning system (indirect effect influenced by the AC system's efficiency).

In this study we provide a comparative evaluation of the COPs of R134a and CO_2 systems using NIST's semi-theoretical vapor compression model, CYCLE-11.UA, and derived from it the transcritical cycle model, CYCLE-11.UA-CO_2. We strived to consider all significant refrigerant and system-related factors, and, consequently, we believe that the resulting evaluation of R134a and CO_2 is more equitable than experimental evaluation that could be obtained within reasonable time and resources spent. Since a refrigerant's performance in a system is strongly affected by hardware design, a comparison of different refrigerants based on laboratory experiment may be significantly affected by hardware design as well. For this reason, even if attempted, a fair comparison of performance potentials of different refrigerants is difficult to derive from laboratory testing, particularly when properties of the studied refrigerants are drastically

different. Using the two related simulation models, we avoided the constraints of experimental hardware but had enough modeling detail to account for unique properties of the refrigerants considered.

2. Literature review

Carbon dioxide was widely used as a refrigerant during the last part of the 19th century and well into the 20th century, however, it fell out of use after the introduction of CFCs in the early 1930s. In the early 1990's, Lorentzen and Pettersen [1] initiated a renewed interest in CO_2 because of its potential to address the environmental problems of ozone depletion and global warming. An intense research effort in CO_2 since then is evidenced in Pettersen and Aarlien [2], Kruse et al. [3], and Strømmen et al. [4]. In successive studies, Lorentzen and Pettersen [5] and Pettersen [6] developed and tested a prototype CO_2 automotive air conditioning system. They used, as a reference, a commercially available R12 automotive air-conditioning system and built a prototype CO_2 system of comparable cooling capacity. The CO_2 system had a liquid-line/suction-line heat exchanger (llsl-hx) to transfer heat between the high-pressure CO_2 leaving the gas cooler and the low-pressure CO_2 leaving the evaporator. The expansion valve was controlled manually. To match the cooling capacity, the displacement volume and speed of the compressor were adjusted. The external dimensions of the air-to-refrigerant heat exchangers were nearly identical for both systems; however, the CO_2 evaporator had 25% larger air-side surface than the R12 evaporator, and the CO_2 gas cooler had 34% larger air-side surface than the R12 condenser. The authors demonstrated that the CO_2 system had comparable performance to the R12 system.

From 1994 to 1997, five European automotive manufacturers and four European automotive suppliers participated in the RACE (refrigeration and automotive climate systems under environmental aspects) project to investigate the feasibility of CO_2 as a refrigerant in automotive air conditioning systems. Gentner [7] presented some results of this experimentally based project showing that CO_2 systems give acceptable cooling capacity, fuel consumption, and lower TEWI, when compared to an R134a system. He noted that the CO_2 system requires additional space to house the llsl-hx, but that the additional weight of the CO_2 air conditioner has no remarkable influence on fuel consumption. Gentner concluded that CO_2 holds promise as an alternative refrigerant for mobile air conditioning applications. He recognized that the automotive industry should continue development until CO_2 systems obtain comparable performance to R134a ones in all relevant aspects.

Bullock [8] theoretically analyzed performance of CO_2 as a refrigerant in a vapor compression cycle with the condenser temperature reaching the critical temperature. His results showed that the CO_2 system is less efficient than the R22 system by 30% in the cooling mode and by 25% in the heating mode. He concluded that to obtain mid-level efficiency of typical unitary equipment, the CO_2 system would require an efficient expander and significantly improved compressor and heat exchangers.

Hwang and Radermacher [9] theoretically compared the performance of R22 and CO_2 for water-heating and water-chilling applications. To this end, they developed and used a vapor-compression cycle model for R22 and a transcritical cycle model for CO_2. They concluded that water-heating is a promising application for CO_2 since its performance is approximately 10% better than R22 across a wide range of ambient temperatures. They also noted that an opportunity exists to reduce the size and weight of CO_2 heat exchangers while maintaining equal performance to R22 by properly designing the CO_2 heat exchangers to take advantage of the CO_2 thermophysical properties.

McEnaney et al. [10,11] presented experimental results for a prototype CO_2 system and a commercially available R134a automotive air conditioner. The CO_2 system employed a llsl-hx and a manual metering valve. The CO_2 evaporator and gas cooler were new generation microchannel heat exchangers developed by Pettersen et al. [12] (Hrnjak [13]) while the R134a heat exchangers where of conventional technology. The external volumes of the evaporators were identical for both systems with the CO_2 evaporator having 20% larger air-side surface area. The CO_2 gas cooler had 23% lower external volume and 28% lower air-side surface than the R134a condenser. The test results indicated that the prototype CO_2 system provided a comparable performance to the current production R134a system for both steady-state and cycling operation.

Boewe et al. [14] investigated the impact of the llsl-hx on the COP and capacity of a CO_2 air conditioner. They performed experiments without the llsl-hx and with three different heat exchangers: 1.0, 1.5, and 2.0 m in length (0.5, 0.7, and 0.9 kg by weight, respectively). The use of the llsl-hx increased both the cooling capacity and COP, though at the expense of increased temperatures at the compressor discharge. For idling conditions, the COP increased by 26% and the cooling capacity increased by 10%. In all the idling cases, the optimum pressure (corresponding to the maximum COP) resulted in a compressor discharge temperature below 140°C (materials permissible limit). For tests performed for driving conditions, the optimum pressure was not attained because it would result in compressor discharge temperatures exceeding 140°C. Therefore, the practical use of the llsl-hx has an effectiveness limit imposed by the compressor discharge temperature. A study by Preissner et al. [15] showed that the impact of the llsl-hx on the COP of the

R134a system is smaller than that found for CO_2. They measured COP and cooling capacity increases in the range of 5–10% at 40°C and a compressor speed of 1000 RPM.

Preissner et al. [16] presented experimental results for prototype CO_2 and R134a automotive air conditioners. The major difference between this study and previous ones is that the R134a evaporator and condenser were prototype heat exchangers based on the latest technology (similar technology to the CO_2 heat exchangers), and a llsl-hx was employed in the R134a system (not just in the CO_2 system as in previous studies). Their major findings were that the capacity of the CO_2 system ranged from 13% lower to 20% higher as compared to the R134a system, and the COP of the CO_2 system ranged from 11 to 23% lower as compared to the R134a system.

Robinson and Groll [17] studied theoretically the performance of the transcritical CO_2 cycle with and without an expansion turbine and compared it to a subcritical R22 cycle. Their major findings were that (1) the COP of the CO_2 work recovery cycle without internal heat exchange is 87–146% of the COP of the conventional R22 cycle, (2) the COP of the CO_2 cycle with internal heat exchange is 72–118% of the conventional R22 cycle, and (3) the use of a work recovery device in conjunction with a llsl-hx does not combine the two effects but tends to reduce the COP of the CO_2 cycle by up to 8%.

Bhatti [18] explored several possibilities to enhance the COP of the R134a system. The augmentation strategies included an increase in compressor efficiency, increase in condenser effectiveness, decrease in evaporator air-side pressure drop by improved condensate removal, and a decrease in oil circulation. With these enhancements, Bhatti argued that an improved R134a system is the most pragmatic automotive air conditioning system to address environmental concerns.

Zietlow et al. [19] performed an experimental study with the aim to improve the COP of a commercially available R134a system. They installed a high-efficiency scroll compressor, a thermostatic expansion valve in place of the short-tube restrictor, and a microchannel heat exchanger that was configured to include a receiver and subcooling section. The evaporator was of a conventional plate-fin design for both the base and improved systems. The results showed a 28% lower compressor power consumption and a 24% increase in the COP as the cooling capacities were maintained within 10% of the original value by regulating the compressor speed.

From this brief literature review, we can observe that the theoretical COP of a CO_2 system is lower than the theoretical COP of an R134a system, while some studies experimentally demonstrated that a CO_2 system could provide the performance level of a current-production R134a system. The studies that reported equivalent performance were based on tests of CO_2 and R134a systems, which were not equivalent component-wise. The use of the llsl-hx is the most obvious difference between the two systems. Except for the study of Preissner et al. [16], the use of different-technology heat exchangers is also a very significant difference because different air-side heat-transfer resistances (coupling of heat transfer coefficient and heat transfer area) may be an important factor affecting the air-to-refrigerant heat-transfer process and the system's COP.

The lower improvement of the COP for R134a than for CO_2 due to the llsl-hx [14,15] may not always justify the cost of installation or the additional package space in the R134a system. However, the benefit-to-cost ratio for using microchannel heat exchangers can be expected to be similar for both refrigerants. For these reasons, in this study we included the llsl-hx only for the CO_2 system but provided the same technology refrigerant-to-air heat exchangers for both refrigerants.

3. Simulation models

3.1. Modeling approach

We used two related simulation models CYCLE-11.UA and CYCLE-11.UA-CO_2. CYCLE-11.UA is a semi-theoretical model for evaluating performance of refrigerants or refrigerant mixtures in the vapor compression cycle [20,21]. The model performs simulations for user-specified temperature profiles of the heat source and heat sink. The simulated system includes the compressor, evaporator, condenser, isenthalpic expansion device, and llsl-hx. The evaporator and condenser are represented by their UA values, which is a product of the overall heat-transfer coefficient (U) and heat-transfer area (A). The llsl-hx is represented by its effectiveness. The user must specify either cross-flow, counter-flow, or parallel-flow configuration for the evaporator and condenser, with refrigerant superheat and subcooling, where appropriate. The model employs FORTRAN subroutines from REFPROP 6.01 [22] to calculate refrigerant thermophysical properties.

CYCLE-11.UA-CO_2 (Brown and Domanski, [23]) is an adaptation of CYCLE-11.UA to the carbon dioxide transcritical cycle. The model uses Span and Wagner [24] routines to calculate thermodynamic properties and calculates thermal conductivity and viscosity based on Vesovic et al. [25]. For surface tension, we developed a correlation from values given in ASHRAE Fundamentals [26]. Because of transcritical operation, the input to the model includes the gas cooler pressure. Alternatively, at the user's option, CYCLE-11.UA-CO_2 can optimize the gas cooler pressure to maximize the COP.

Both models employ the same convergence logic, which establishes a thermodynamic loop with respect to the heat sink and source temperatures while satisfying

constraints imposed by the input data. For the evaporator, condenser, and gas cooler, the models aim to obtain agreement between the ΔT calculated using refrigerant and external heat-transfer fluid (HTF) properties, and the ΔT calculated from the basic heat transfer relation given in Eq. (1).

$$\dot{Q}_{hx} = \dot{m}_r \Delta i_r = UA \Delta T_{hx} \qquad (1)$$

The ΔT calculated using refrigerant and HTF properties is a harmonic mean of the ΔTs for the individual sections (e.g. two-phase and superheated refrigerant). Non-linearities in the refrigerant temperature profiles are accounted for by dividing individual sections into smaller segments, as necessary [20]. Validation of CYCLE-11.UA and CYCLE-11.UA-CO$_2$ are presented in Domanski et al. [27] and Brown and Domanski [23], respectively.

3.2. Compressor

We assumed an open-type compressor and modeled it using empirical correlations for volumetric and isentropic efficiencies developed from published data. We modeled volumetric efficiency for CO_2 and R134a compressors with the following correlation:

$$\eta_V = 0.8263 \left[1 - 0.09604 \left(\theta^{\frac{1}{\gamma}} - 1 \right) \right] \qquad (2)$$

We obtained this correlation by curve-fitting the data of McEnaney et al. [11] and Park et al. [28] for a CO_2 compressor and an R134a compressor, respectively. Regarding the isentropic efficiency, we curve-fitted the isentropic efficiency curve presented by Rieberer and Halozan [29] for a CO_2 compressor, which is based on experimental data of four authors. In the obtained correlation, the isentropic efficiency is a function of the ratio of compressor discharge and suction pressures, θ. For a pressure ratio greater than 2, this correlation has the following form:

$$\eta_s = 0.9343 - 0.04478 \, \theta \qquad (3)$$

Several researchers [5,6] postulated that a lower pressure ratio inherently results in higher compressor efficiency. Following this postulate, the CO_2 compressor should have a higher isentropic efficiency than the R134a compressor because the pressure ratio for a CO_2 system is on the order of three whereas for an R134a system it is on the order of five to seven. The opposing view is that the higher efficiencies measured for CO_2 compressors compared to the current-production R134a compressors are rather a result of compressor design itself. Given this controversy, we decided to use Eq. (3) for both CO_2 and R134a compressors to be consistent

with experimental studies in which CO_2 compressors were found to be more efficient than R134a compressors and to give CO_2 a possibly valid credit.

3.3. Refrigerant-to-air heat exchangers (evaporator, condenser, gas cooler)

All three refrigerant-to-air heat exchangers had a cross-flow configuration. We accounted for the impact of thermophysical properties on the refrigerant heat-transfer coefficient and the pressure drop on a relative basis. The simulation scheme started with a simulation at a reference-point operating condition for which we imposed UA values to obtain realistic temperature differences between the refrigerant and HTFs. Since the total resistance to heat transfer is comprised of the resistance on the HTF side, resistance due to heat exchanger material, and resistance on the refrigerant side ($R_{hx} = R_{HTF} + R_{tube} + R_r$), the following equation holds:

$$R_{HTF} + R_{tube} = \frac{1}{UA_{hx}} - \frac{1}{h_r A_r} \qquad (4)$$

where $1/UA_{hx} = R_{hx}$ and $1/h_r A_r = R_r$. For the reference-point operating condition with imposed UA_{hx} and A_r, and calculated value of refrigerant heat-transfer coefficient, h_r, the left-hand side of Eq. (4) can be obtained. This value can then be used for other operating conditions or another refrigerant to simulate UA_{hx} according to Eq. (5):

$$UA_{hx} = \frac{1}{R_{HTF} + R_{tube} + \dfrac{1}{h_r A_r}} \qquad (5)$$

We used this procedure starting with a simulation for the carbon dioxide system at a selected reference-point operating condition and applied Eq. (5) to calculate UA values for other simulations for both CO_2 and R134a systems. This representation of the heat exchangers assured that the heat exchangers in the CO_2 and R134a systems had the same air-side heat-transfer resistances, which are typically the dominant ones. At the same time, this method accounted for differences in refrigerant-side heat-transfer coefficients between CO_2 and R134a and for different operating conditions.

CYCLE-11.UA and CYCLE-11.UA-CO$_2$ employ in-tube flow correlations to calculate refrigerant-side heat-transfer coefficients. For the evaporation heat-transfer coefficient of R134a, CYCLE-11.UA used the Thome et al. [30] correlation, because it was validated with diverse fluids, including R134a. For calculating the CO_2 evaporation heat-transfer coefficient, CYCLE-11.UA-CO$_2$ uses the CO_2-specific correlation developed by Hwang et al. [31]. This correlation was derived from the Bennett-Chen [32] correlation to fit Bredesen et al. [33] CO_2 data.

The reason for developing this CO_2-specific correlation was the fact that commonly accepted heat-transfer correlations under-predict Bredesen et al. [33] data by approximately a factor of two.

For calculating the condensation heat-transfer coefficient of R134a, CYCLE-11.UA used the relatively old correlation of Shah [34] because it shows good agreement with experimental data for various fluids, as reported by Eckels et al. [35]. For calculating the gas cooler heat-transfer coefficient, we followed the suggestion of Pitla et al. [36] and provided CYCLE-11.UA-CO_2 with the correlation of Krasnoshchekov et al. [37]:

$$Nu_w = Nu_{PK}\left(\frac{\rho_w}{\rho_b}\right)^n \left(\frac{\overline{cp}}{(c_p)_w}\right)^q$$

$$\overline{cp} = \frac{i_b - i_w}{T_b - T_w}$$

$$q = b\left(\frac{\overline{cp}}{(c_p)_w}\right)^j \tag{6}$$

NU_{PK} is the Nusselt number given by the Petukhov–Kirillov's correlation [38], and is given in Eq. (7).

$$Nu_{PK} = \frac{\xi/8 Re Pr}{12.7\sqrt{\xi/8}(Pr^{2/3} - 1) + 1.07} \tag{7}$$

Re is the Reynolds number, Pr is the Prandtl number, and ξ is the friction coefficient given by the Flonenko correlation [38], and is given in Eq. (8).

$$\xi = (0.79 \ln(Re) - 1.64)^{-2} \tag{8}$$

Krasnoshchekov et al. [37] present the coefficients n, b, and j in graphical form. We have developed correlations (given in Appendix A) based on their data and have incorporated them into the model. The gas cooler is divided into thirty equal-temperature interval segments for which the local CO_2 heat-transfer coefficient is calculated. The mean of these values is used as an average CO_2 heat-transfer coefficient in the gas cooler.

Pressure drop in the heat exchangers is evaluated on a relative basis using a scheme similar to the one for calculating the *UA* values [21]. Since the gravitational and momentum components are small, the model calculates only the frictional pressure drop. To predict two-phase pressure drop (in-tube evaporation of CO_2 and R134, and condensation of R134a), the model uses the frictional term of the modified Pierre correlation [39]. For the transcritical CO_2 cooling process, the model calculates the frictional pressure drop using the conventional Blausius single-phase correlation for turbulent in-tube flow, $f = 0.184 Re^{-0.2}$, as given by Kakaç and Liu [38] (the dynamic pressure drop typically constitutes less than 1% of the total pressure drop). CYCLE-11.UA-CO_2 calculates pressure drop for each of 30 gas cooler segments. The total pressure drop is then simply the sum of these individual pressure drops.

3.4. Liquid-line/suction-line heat exchanger

The llsl-hx is of a counter-flow configuration and employs a user-specified effectiveness to model its thermal performance. The pressure drops on both the high-pressure and low-pressure sides of the llsl-hx are simulated in the same manner as for the gas cooler.

3.5. Expansion device

Both cycle models treat the expansion process as isenthalpic. In the systems simulated in this study, the expansion device is a variable flow device that controls the high-side pressure. The R134a simulations approximated the use of a TXV by holding constant the evaporator superheat and condenser subcooling at 5°C. For the CO_2 transcritical cycle, heat rejection is above the critical point in most cases. Thus subcooling at the gas cooler outlet cannot be specified, and different transcritical cycles with different COPs can be established depending on the gas cooler pressure. Optimizing this pressure for maximum COP was discussed by Pettersen [6], among others. McEnaney et al. [11] further pointed out the practical high-side limitation for the gas cooler pressure due to temperature limitations of the compressor materials, which in their case was 140°C. Considering these issues, CYCLE-11.UA-CO_2 includes the following options for the gas cooler pressure: (1) imposed, (2) optimized for maximum COP, and (3) optimized for maximum COP overridden by the 140°C compressor discharge temperature limit.

4. Simulations

4.1. Systems studied and operating conditions

The CO_2 system consisted of a compressor, gas cooler, llsl-hx, variable opening expansion device, and evaporator. The components and system were selected to match the system studied experimentally by McEnaney et al. [11]. The compressor had the same displacement volume. The gas cooler and evaporator had the same physical characteristics, e.g. refrigerant passage diameters, number of circuits, and air-side surface.

The R134a system had the configuration of a current-production automotive air conditioner. It consisted of a compressor, condenser, variable opening expansion device, evaporator, but did not include a llsl-hx. Considering the air-side, the condenser was the same heat exchanger as the CO_2 gas cooler. On the refrigerant side, the number of refrigerant passages was the same, but

the circuitry was rearranged to obtain a pressure drop comparable to that of a conventional R134a system. Similarly, the R134a evaporator was derived from the CO_2 evaporator by rearranging the circuitry. In both cases, rearranging the circuitry reduced the pressure drop penalty at the expense of a lower refrigerant-side heat-transfer coefficient. The R134a compressor had an increased displacement volume to obtain the same cooling capacity as the CO_2 system at 1000 RPM and an ambient temperature of 43.3°C.

Three air temperatures at the condenser/gas cooler inlet (32.2, 43.3 and 48.9°C) and one temperature at the evaporator inlet (26.7°C) comprised the operating conditions. Compressor speeds of 1000 and 3000 RPM represented low-speed and high-speed operation.

We used one 1000 RPM test and one 3000 RPM CO_2 test as two independent reference points for deriving the air-side heat-transfer resistances of the refrigerant-to-air heat exchangers for low-speed and high speed operation, respectively, and we used these resistances in the heat exchanger simulation schemes for the CO_2 and R134a systems. This approach offered more accurate predictions considering that the air-side heat-transfer coefficient varies considerably with compressor speed. For the gas cooler, the air-side heat-transfer coefficient is affected by different volumetric flow rates of air. For the evaporator, different refrigerant temperatures for different compressor speeds result in different moisture

removal rates and thus different heat-transfer coefficients. All of these effects on the air side are difficult to simulate in a semi-theoretical model. The selected inlet air temperatures for the 1000 and 3000 RPM reference test points were 43.3°C for the gas cooler and 26.7°C for the evaporator.

Fig. 1 shows the CO_2 transcritical cycle and the R134a subcritical cycle obtained at an ambient temperature of 43.3°C for 1000 compressor RPM. The significantly higher discharge temperature and larger temperature change for CO_2 than for R134a in the high-pressure heat exchanger are the most visible differences. The large CO_2 glide is the reason for significant temperature mismatch because the refrigerant-to-air heat exchangers are cross-flow. The figure also shows that the temperature approach for the CO_2 gas cooler is lower than for the R134a condenser, which benefits the COP of carbon dioxide; however, even qualitative visual examination suggests that the benefit of a lower temperature approach cannot compensate for the penalty due to the air/CO_2 temperature mismatch.

Fig. 2 shows COP as a function of ambient temperature and compressor speed. At 1000 RPM for an ambient condition of 32.2°C, the R134a system's COP is approximately 21% higher than the CO_2 system's COP. The COP gap increases to 29% at 43.3°C and to 34% at 48.9°C. At 3000 RPM for an ambient condition of 32.2°C, the R134a system's COP is approximately 42%
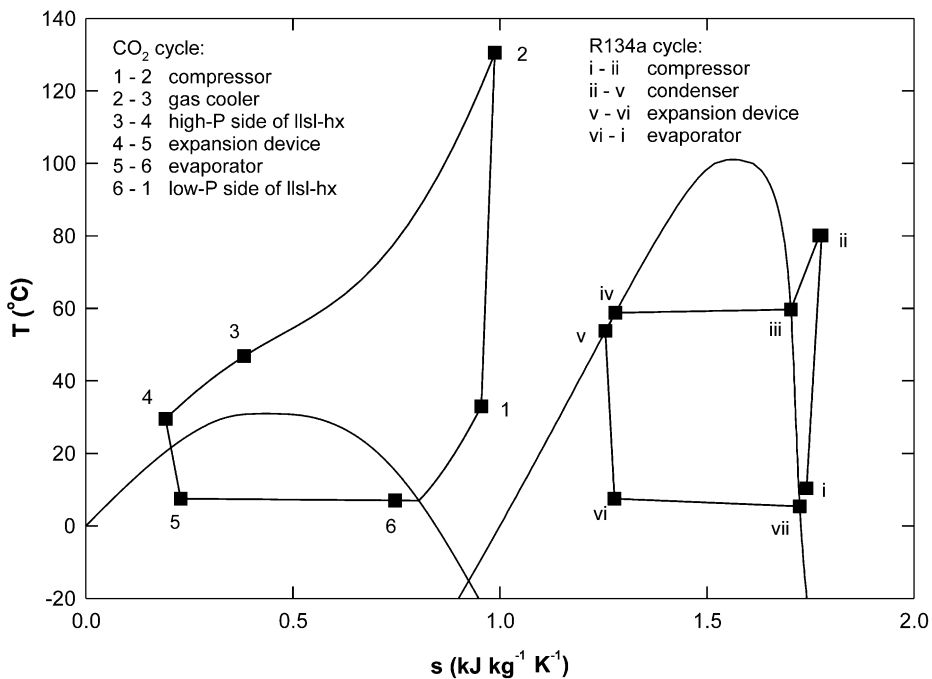

Fig. 1. CO_2 transcritical cycle and the R134a subcritical cycle at an ambient temperature of 43.3°C and 1000 compressor RPM.

Fig. 1. Cycle transcritique du CO₂ et cycle sous-critique de R134a à une température ambiante de 43,3°C et une vitesse du compresseur de 1000 tours/minute.
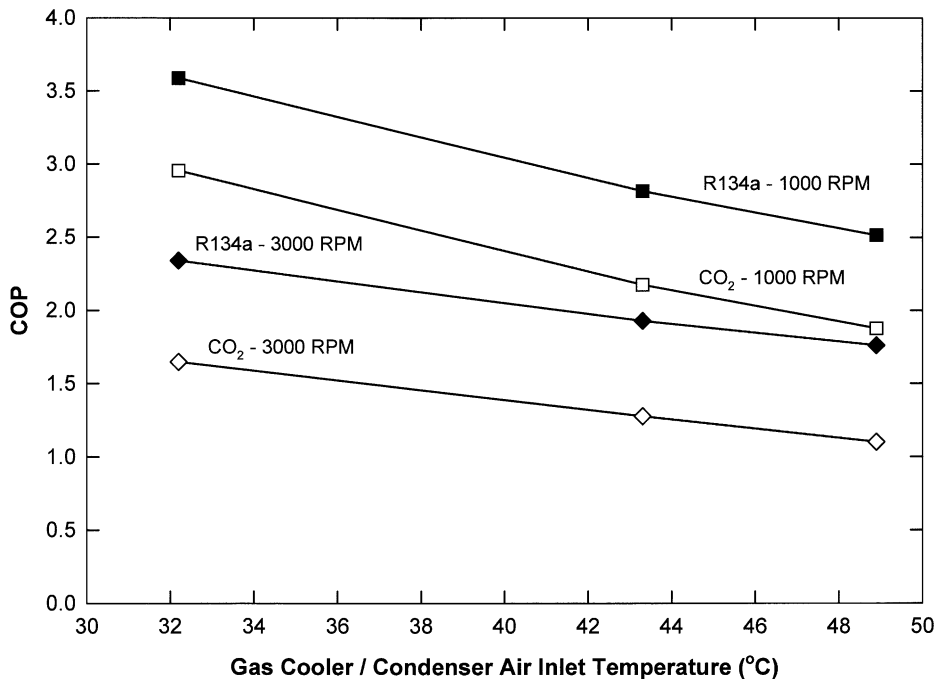
Fig. 2. COP comparison between CO_2 and R134a air conditioning systems.

Fig. 2. Comparaison des COP des systèmes de conditionnement d'air au CO_2 et au R134a.

higher than that of the CO_2 system. The COP gap increases to 51% at 43.3°C and to 60% at 48.9°C.

Fig. 3 shows cooling capacity as a function of ambient temperature and compressor speed. At 1000 RPM, capacities of both systems are similar because of the imposed capacity match at an ambient temperature of 43.3°C. At 3000 RPM, capacities of both systems happen to match at an ambient temperature of 32.2°C. At higher ambient temperatures, the R134a system has a higher capacity by 3.6% at 43.3°C and by 7.2% at 48.9°C. The interdependence between capacity and COP for different compressors speeds is captured in Fig. 4.

Fig. 5 shows compressor power as a function of ambient temperature and compressor speed. At 1000 RPM for an ambient temperature of 32.2°C, the CO_2 system's compressor power is approximately 20% higher than the R134a system's compressor power. The gap increases to 29% at 43.3°C and to 36% at 48.9°C. At 3000 RPM for an ambient temperature of 32.2°C, the CO_2 system's compressor power is approximately 42% higher than the R134a system's compressor power. The gap increases to 46% at 43.3°C and to 49% at 48.9°C.

We can gain an insight into the CO_2 and R134a systems' irreversibilities reviewing the entropy generation information shown in Fig. 6 for the refrigerant-to-air heat exchangers and for both systems. The figure uses an entropy-per-capacity ordinate in recognition of the fact that an absolute scale would result in different entropy generations for two systems of the same efficiency if

their capacities were different. The entropies generated in the CO_2 and R134a evaporators are similar, with the CO_2 evaporator producing a smaller amount of entropy. This result is due to the superior transport properties of CO_2. On the other hand, the entropy generation in the CO_2 gas cooler is much greater than in the R134a condenser. Here, the large CO_2 temperature glide (approximately 80 versus 25°C for R134a) and the larger amount of heat needed to be rejected by the CO_2 gas cooler than by the R134a condenser (3.7–11.7% higher for 1000 compressor RPM and 12.7–13.4% higher for 3000 compressor RPM) causes a significant amount of entropy generation (heat-transfer irreversibilities) in the cross-flow heat exchanger. The large amount of entropy generation in the gas cooler is primarily responsible for the higher total entropy generation for the CO_2 system. We may note that large entropy generation is unavoidable in a cross-flow heat exchanger for high-glide fluids. Hence, the cross-flow gas cooler will negatively affect the performance of the transcritical CO_2 cycle while application of a counter-flow gas cooler may offer COP advantage if glide matching with the external heat-transfer fluid is obtained.

5. Simulation trade-offs

It is proper to note the features in the simulation models that were introduced to account for peculiarities
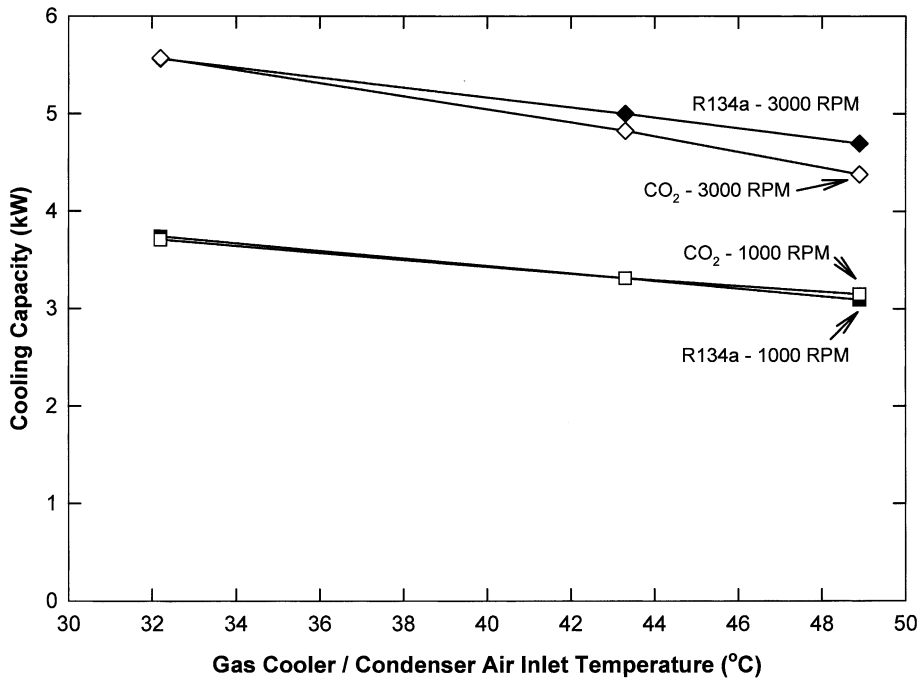
Fig. 3. Cooling capacity comparison between CO_2 and R134a air conditioning systems.

Fig. 3. Comparaison des puissances frigorifiques des systèmes de conditionnement d'air au CO_2 et au R134a.
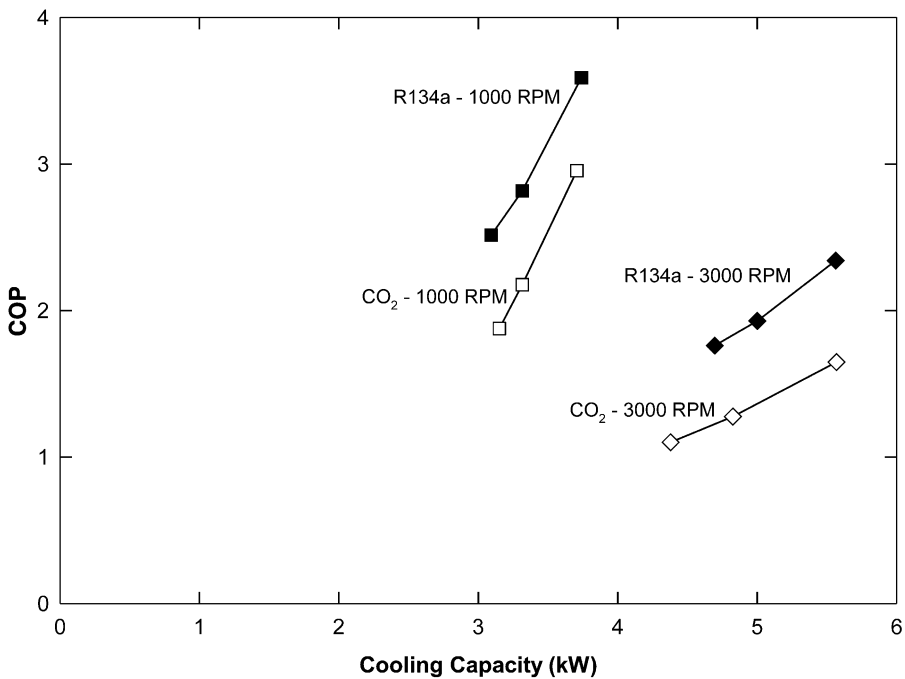

Fig. 4. COP comparison versus cooling capacity between CO_2 and R134a air conditioning systems.

Fig. 4. Comparaison du COP et des puissances frigorifiques des systèmes de conditionnement d'air au CO_2 et au R134a.
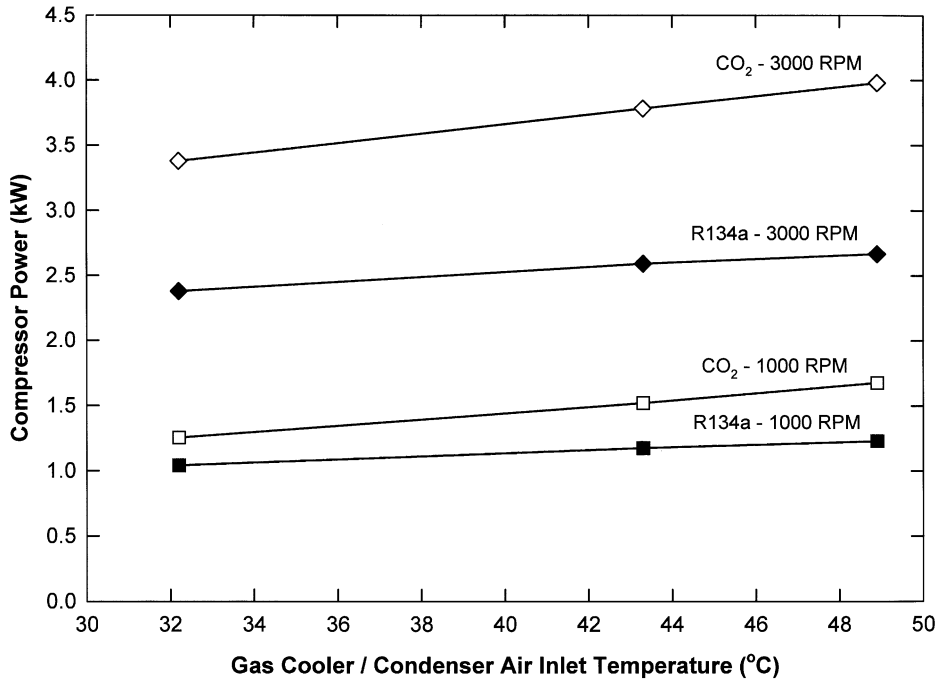
Fig. 5. Compressor power consumption comparison between CO_2 and R134a air conditioning systems.

Fig. 5. Comparaison de la consommation d'énergie du compresseur des systèmes de conditionnement d'air au CO_2 et au R134a.
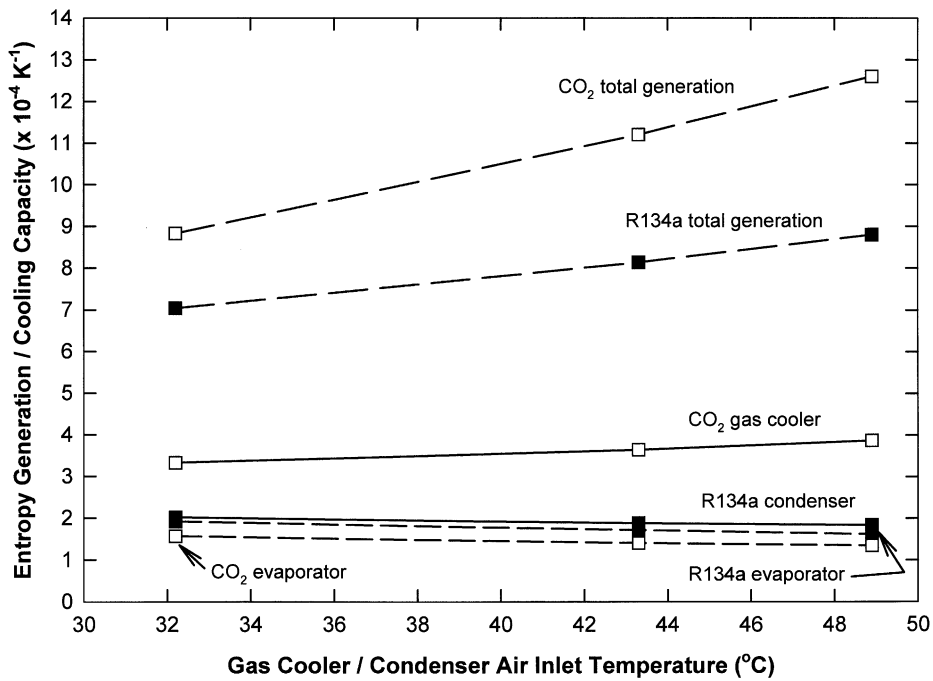

Fig. 6. Comparison of entropy generation per unit cooling capacity for CO_2 and R134a air conditioning systems at 1000 compressor RPM.

Fig. 6. Comparaison de la génération d'entropie par unité de puissance frigorifique des systèmes de conditionnement d'air au CO_2 et au R134a à des vitesses du compresseur de 1000 tours/minute.
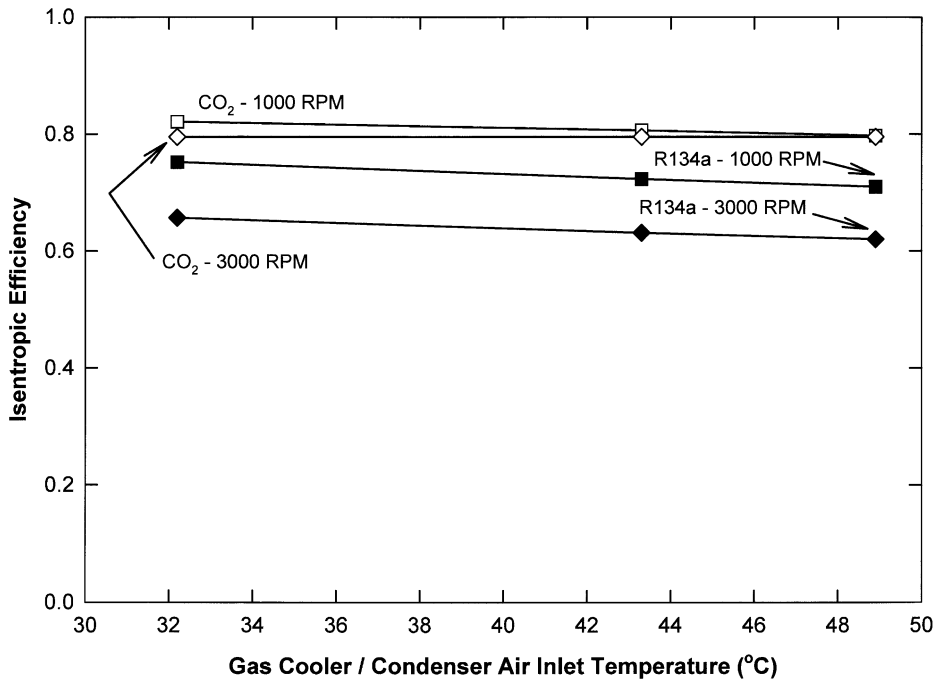
Fig. 7. Compressor isentropic efficiency comparison between CO_2 and R134a air conditioning systems.

Fig. 7. Systèmes de conditionnement d'air au CO_2 et au R134a : comparaison de l'efficacité isentropique du compresseur.
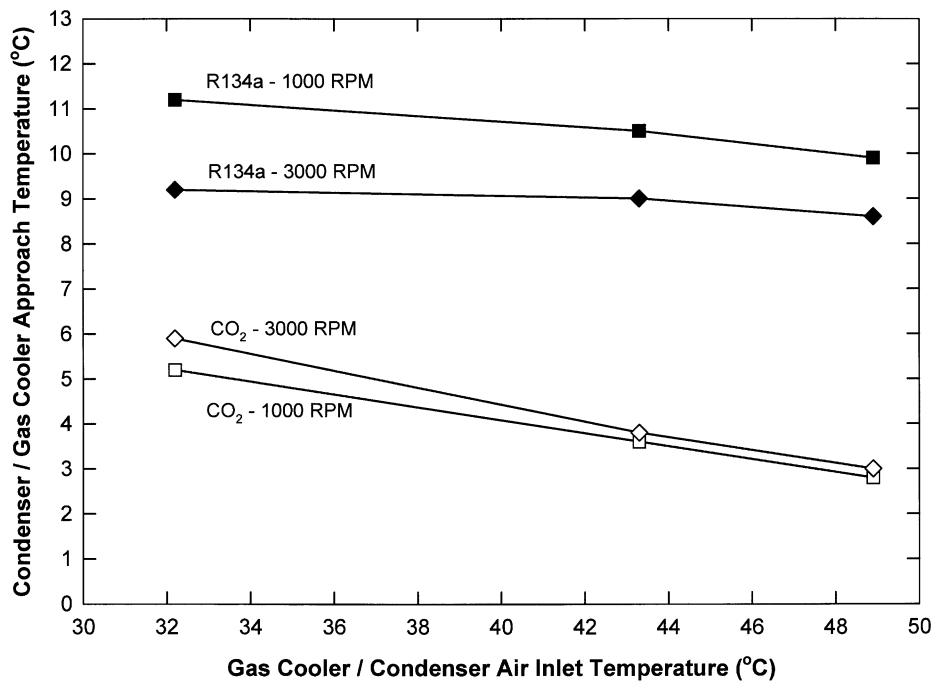

Fig. 8. Condenser/gas cooler approach temperature comparison between CO_2 and R134a air conditioning systems.

Fig. 8. Systèmes de conditionnement d'air au CO_2 et au R134a : approche utilisant la comparaison des températures du condenseur et du refroidisseur de gaz.

of the transcritical CO_2 cycle and to point out the limitations in the simulations that might benefit one fluid over the other. We provided a benefit to the CO_2 compressor for its lower compression ratio. Fig. 7 shows compressor isentropic efficiency as a function of ambient temperature and compressor speed. Because of the CO_2 system's lower compressor pressure ratio, the CO_2 compressor has a higher isentropic efficiency as given by Eq. (2). In this way, CO_2 receives the credit postulated by some researchers. At 1000 RPM for ambient temperatures of 32.2, 43.3 and 48.9°C, the CO_2 compressor's isentropic efficiencies are 82.1, 80.6 and 79.7%, respectively. For the same compressor speed and ambient temperatures, the R134a compressor's isentropic efficiencies are 75.2, 72.3 and 71.0%, respectively. At 3000 RPM for ambient temperatures of 32.2, 43.3 and 48.9°C, the CO_2 compressor's isentropic efficiency stays the same at 79.5% due to reaching the 140°C restriction on the compressor discharge temperature. For the same compressor speed and ambient temperatures, the R134a compressor's isentropic efficiencies are 65.7, 63.1 and 62.0%, respectively.

The simulations agree with Pettersen's observations [40], that a CO_2 gas cooler can obtain a closer approach temperature than an R134a condenser for equal size heat exchangers, as shown in Fig. 8. The approach temperature in the CO_2 gas cooler is 3.0–5.8°C, while for the R134a condenser the range is 8.5–11.2°C. The closer approach temperature, however, did not overcome the thermodynamic penalty associated with the large temperature glide resulting in high entropy generation, as previously discussed.

The R134a evaporator and condenser were derived from CO_2 microchannel heat exchangers by increasing the number of circuits to obtain reasonable pressure drops (at the expense of reduced refrigerant-side heat-transfer coefficients). This may favor the R134a system over the CO_2 system since we did not account for the increased maldistribution that would occur in the R134a heat exchangers due to the larger number of circuits and the greater difference in the vapor-to-liquid density ratio for R134a versus CO_2. On the other hand, R134a would benefit from the use of a llsl-hx [15,41]. Also, the R134a system is not receiving the benefit of better humidity control and to some degree a higher air-side heat-transfer coefficient associated with moisture condensation. These two effects are due to a lower R134a evaporator temperature versus CO_2 by as much as 1.3°C.

6. Conclusions

We evaluated performance merits of CO_2 and R134a automotive air conditioners using vapor compression and transcritical cycle simulation models. We considered a current-production configuration for the R134a system (compressor, condenser, expansion device, and evaporator) and a CO_2 system, which was additionally equipped with the llsl-hx. In our analysis, the R134a evaporator and condenser were derived from the CO_2 refrigerant-to-air heat exchangers by modifying the refrigerant circuits to obtain reasonable R134a pressure drops. We accounted for the better transport properties of CO_2 and its higher compressor isentropic efficiency due to a lower compression ratio. Also, our simulations credited CO_2 by predicting a lower approach temperature in the gas cooler as compared to that in the R134a condenser.

The analysis shows CO_2 having an inferior COP to R134a. The COP disparity depends on compressor speed (system capacity) and ambient temperature; the higher are the speed and ambient temperature, the greater is the COP difference. For 1000 compressor RPM, the COP for CO_2 ranged from being lower by 21% at 32.2 C to 34% at 48.9 C. At the same speed and lower ambient temperature, this COP disparity will be lower; however, at higher speeds and ambient temperatures, it will be greater. Hence, better transport properties and better compressor isentropic efficiency of CO_2 did not compensate for its thermodynamic disadvantage compared to R134a when equivalent heat exchangers are used for both refrigerants, even if a llsl-hx is used in the CO_2 cycle to reduce throttling irreversibilities.

The entropy generation calculations indicated that CO_2 has a somewhat better performance than R134a in the evaporator, but has significantly poorer performance in the gas cooler than R134a in the condenser. The large CO_2 temperature glide in the gas cooler (approximately 80°C versus 25°C for R134a) and the larger amount of heat needed to be rejected by the CO_2 gas cooler than the R134a condenser are responsible for the higher entropy generation. This large entropy generation in the gas cooler is the primary cause for the lower CO_2 performance and is unavoidable in air-to-refrigerant cross-flow heat exchangers.

Appendix

The coefficients that appear in Kransnoshchekov et al.'s [37] correlation in Eq. (6) are given by:

$$n = \frac{-48.3865106}{(P/P_{cr})} - 184.4985\log_{10}(P/P_{cr})$$
$$+ 48.5062915(P/P_{cr})^{0.74} \tag{A1}$$

$$b = \frac{-9.0586}{(P/P_{cr})} - 27.27997\log_{10}(P/P_{cr})$$
$$+ 9.670075\sqrt{(P/P_{cr})} \tag{A2}$$

$$j = -9.4638845 \times 10^{-6}(P/P_{cr})^{15} + \frac{0.24072314}{(P/P_{cr})^6}$$
$$+ \frac{0.089613245}{(P/P_{cr})^{15}} \tag{A3}$$

where P is the pressure and P_{cr} is the critical pressure. Note: there is no physical significance to the functional form of these equations; they simply were developed to fit Krasnoshchekov et al.'s data [37].

References

[1] Lorentzen G, Pettersen J. New possibilities for non-CFC refrigeration. In Proceedings of the IIR International Symposium on Refrigeration, Energy, and Environment, Trondheim, Norway, 1992, p. 147–63.

[2] Pettersen J, Aarlien R. Progress in CO_2 vapour compression systems. Thermal Science and Engineering 1998;6(1): 25–34.

[3] Kruse H, Heidelck R, Suss J. The application of CO_2 as a refrigerant. Bulletin of the International Institute of Refrigeration 1999;99-1:2–21.

[4] Strømmen I, Bredesen AM, Eikevik T, Nekså P, Pettersen J, Aarlien R. Refrigeration, air-conditioning, and heat-pump systems for the 21st century. Bulletin of the International Institute of Refrigeration 2000;2000-2:3–18.

[5] Lorentzen G, Pettersen J. A new efficient and environmentally benign system for car air-conditioning. International Journal of Refrigeration 1993;16(1):4–12.

[6] Pettersen J. An efficient new automobile air-conditioning system based on CO_2 vapor compression. ASHRAE Transactions 1994;100(2):657–65.

[7] Gentner H. Passenger car air conditioning using carbon dioxide as refrigerant. In Proceedings of the IIR-Gustav Lorentzen Conference on Natural Working Fluids, Oslo, Norway, 1998, p. 303–13.

[8] Bullock CE. Theoretical performance of carbon dioxide in subcritical and transcritical cycles. In Proceedsings of ASHRAE/NIST Refrigerants Conference, Gaithersburg, Maryland, 1997, p. 20–26.

[9] Hwang Y, Radermacher R. Theoretical evaluation of carbon dioxide refrigeration cycle. HVAC&R Research 1998;4(3):245–63.

[10] McEnaney RP, Boewe DE, Yin JM, Park YC, Bullard CW, Hrnjak PS. Experimental comparison of mobile A/C systems when operated with transcritical CO_2 versus conventional R134A. In Proceedings of the Seventh International Refrigeration Conference at Purdue University, West Lafayette, Indiana, 1998, p. 145–50.

[11] McEnaney RP, Park YC, Yin JM, Hrnjak PS. Performance of the prototype of a transcritical R744 mobile A/C system. SAE International Congress and Exposition, Detroit, Michigan, Paper No. 1999-01-0872, 1999.

[12] Pettersen J, Hafner A, Skaugen G, Rekstad H. Development of compact heat exchangers for CO_2 air-conditioning systems. International Journal of Refrigeration 1998; 21(3):180–93.

[13] Hrnjak PS. Private communication. September, 1999.

[14] Boewe D, Yin J, Park YC, Bullard CW, Hrnjak PS. The role of suction line heat exchanger in transcritical R744 mobile A/C systems. SAE International Congress and Exposition, Detroit, Michigan, Paper No. 1999-01-0583, 1999.

[15] Preissner M, Cutler B, Radermacher R, Zhang CA. Suction line heat exchanger for R134a automotive air-conditioning system. In Proceedings of 2000 International Refrigeration Conference at Purdue, West Lafayette, Indiana, 2000, p. 289–94.

[16] Preissner M, Cutler B, Singanamalla S, Hwang Y, Radermacher R. Comparison of automotive air-conditioning systems operating with CO_2 and R134a. In Proceedings of 4th IIR-Gustav Lorentzen Conference on Natural Working Fluids at Purdue, West Lafayette, Indiana, 2000, p. 185–92.

[17] Robinson DM, Groll EA. Efficiencies of transcritical CO_2 cycles with and without an expansion turbine. International Journal of Refrigeration 1998;21(7):577–89.

[18] Bhatti MS. Enhancement of R134a automotive air conditioning system. SAE International Congress and Exposition, Detroit, Michigan, Paper No. 1999-01-0870, 1999.

[19] Zietlow D, Sharma A, Meyer J. An experimental study of power reduction opportunities for automotive air conditioning systems. In Proceedings of the 20th International Congress of Refrigeration, Sydney, Australia, 1999.

[20] Domanski PA, McLinden MO. A simplified cycle simulation model for the performance rating of refrigerants and refrigerant mixtures. International Journal of Refrigeration 1992;15(2):81–8.

[21] Domanski PA, Didion DA, Mulroy WJ, Parise J. A simulation model and study of hydrocarbon refrigerants for residential heat pump systems. In Proceedings of the IIR Conference on New Applications of Natural Working Fluids in Refrigeration and Air Conditioning, Hanover, Germany, 1994, p. 339–54.

[22] McLinden M, Klein SA, Lemmon EW, Peskin AP. NIST thermodynamic and transport properties of refrigerants and refrigerant mixtures — REFPROP, Version 6.0, NIST Standard Reference Database 23, 1998.

[23] Brown JS. Domanski PA. Semi-theoretical simulation model for a transcritical carbon dioxide mobile a/c system. SAE International Congress and Exposition, Detroit, Michigan, Paper. No. 2000-01-0985, 2000.

[24] Span R, Wagner W. A new equation of state for carbon dioxide covering the fluid region from the triple-point temperature to 1100 K at pressures up to 800 MPa. Journal Physics Chemistry Reference Data 1996;25(6):1509–96.

[25] Vesovic V, Wakeham WA, Olchowy GA, Sengers JV, Watson JTR, Millat J. The transport properties of carbon dioxide. Journal Physics Chemistry Reference Data 1990;19(3):763–808.

[26] ASHRAE. Refrigerant Properties. ASHRAE handbook of fundamentals, 1997.

[27] Domanski PA, Mulroy WJ, Didion DA. Glide matching with binary and ternary zeotropic refrigerant mixtures. Part 2: a computer simulation. International Journal of Refrigeration 1994;17(4):226–30.

[28] Park YC, McEnaney R, Boewe D, Yin JM, Hrnjak PS. Steady state and cycling performance of a typical R134a mobile A/C system. SAE International Congress and Exposition, Detroit, Michigan, Paper No. 1999-01-1190, 1999.

[29] Rieberer R, Halozan H. CO_2 heat pumps in controlled ventilation systems. In Proceedings of IIR- Gustav Lorentzen Conference on Natural Working Fluids, Oslo, Norway, 1998, p. 212–22.

[30] Thome JR. Heat transfer and pressure drop in the dry-out region of in-tube evaporation with refrigerant/lubricant mixtures. ASHRAE RP-800, 1996.

[31] Hwang Y, Kim BH, Radermacher R. Boiling heat transfer correlation for carbon dioxide. In Proceedings of 1997 Heat Transfer Issues in 'Natural' Refrigerants, Center for Environmental Energy Engineering, University of Maryland, College Park, Maryland, 1997, p. 81–95.

[32] Bennett DL, Chen JC. Forced convection boiling in vertical tubes for saturated pure components and binary mixtures. Journal of AIChE 1980;26:454–61.

[33] Bredesen AM, Hafner A, Pettersen J, Nekså P, Aflekt K. Heat transfer and pressure drop for in-tube evaporation of CO_2. In Proceedings of the 1997 Heat Transfer Issues in 'Natural' Refrigerants, Center for Environmental Energy Engineering, University of Maryland, College Park, Maryland, 1997, p. 35–49.

[34] Shah MM. A new correlation for heat transfer during boiling flow through pipes. ASHRAE Transactions 1976;88(1):185–96.

[35] Eckels SJ, Tesene B, Wang Q. In-tube condensation of refrigerants in smooth and enhanced tubes. ASHRAE New Investigator Project, 1998.

[36] Pitla SS, Robinson DM, Groll EA, Ramadhyani S. Heat transfer from supercritical carbon dioxide in tube flow: a critical review. HVAC & R Research 1998;4(3):281–301.

[37] Krasnoshchekov EA, Kuraeva IV, Protopopov VS. Local heat transfer of carbon dioxide at supercritical pressure under cooling conditions. Teplofizika Vysokikh Temperatur 1969; 7(5): 922–30. (English translation: High Temperature (USSR) 7(5): 856–86.)

[38] Kakaç S, Liu H. Heat exchangers: selection, rating, and thermal design. Boca Raton, Florida: CRC Press, 1998 (pp. 90 and 117).

[39] Choi JY, Kedzierski MA, Domanski PA. A generalized pressure drop correlation for evaporation and condensation of alternative refrigerants in smooth and micro-fin tubes. NISTIR 6333, US Department of Commerce, Washington, DC, 1999.

[40] Pettersen J. Carbon dioxide (CO_2) as a primary refrigerant. Centenary Conference of the Institute of Refrigeration. London, 1999.

[41] Domanski PA, Didion DA, Doyle JP. Evaluation of suction line–liquid line heat exchange in the refrigeration cycle. International Journal of Refrigeration 1994;17(7): 487–493.